Supplementary Information

Ferroelectric Domains in Methylammonium Lead Iodide Perovskite Thin-Films

Holger Röhm,[ab†] Tobias Leonhard,[ab†] Michael J. Hoffmann[bc] and Alexander Colsmann[ab]*

a. Light Technology Institute, Karlsruhe Institute of Technology (KIT), Engesserstrasse 13, 76131 Karlsruhe, Germany
b. Material Research Center for Energy Systems (MZE), Karlsruhe Institute of Technology (KIT), Strasse am Forum 7, 76131 Karlsruhe, Germany
c. Institute for Applied Materials – Ceramic Materials and Technologies, Karlsruhe Institute of Technology (KIT), Haid- und-Neu-Strasse 7, 76131 Karlsruhe, Germany
**. Contact: alexander.colsmann@kit.edu*
†. The first two authors contributed equally to this work.

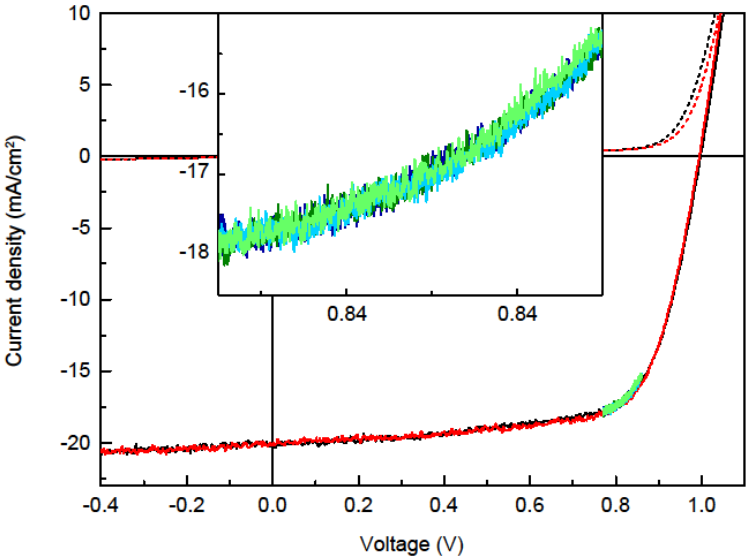

Fig. S1. Almost hysteresis-free *J-V* curves of a typical $MAPbI_3(Cl)$ solar cell in forward (red curve) and reverse (black curve) direction (scanning speed 100mV/s). Inset: The PCE of 14% was derived from forward (dark and light blue) and reverse (dark and light green) semi-steady state measurements (5 mV/s) around the maximum power point. No external electrical poling was conducted prior to the measurement.

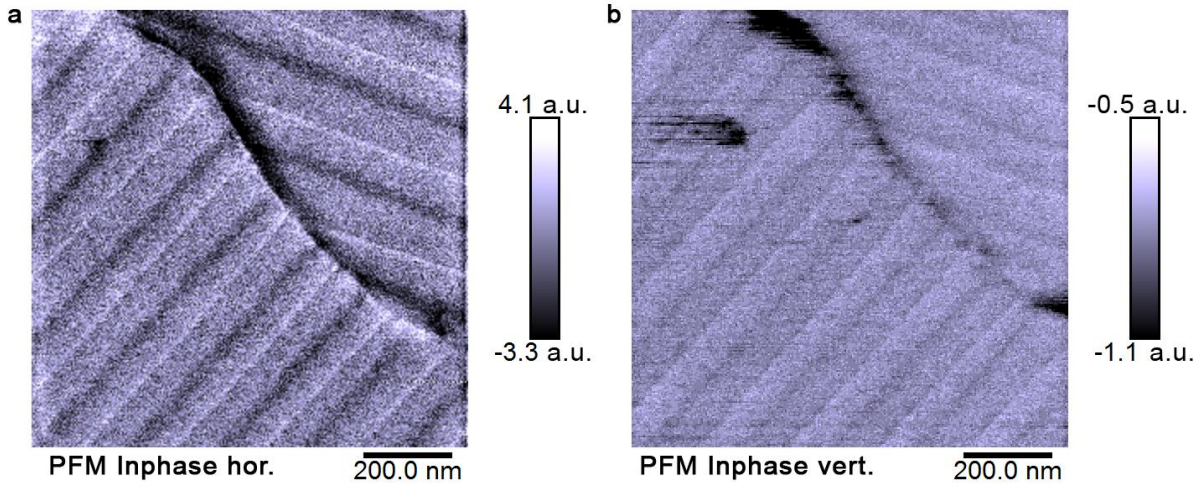

Fig. S2. Comparison of (a) horizontal (in-plane) and (b) vertical PFM signals of a $MAPbI_3(Cl)$ grain boundary. Both channels show the same domain features, whereas different cantilever stiffness for vertical and horizontal deflection hampers quantitative analysis of vertical and horizontal signal magnitudes, respectively. The vertical cantilever response can be influenced by in-plane polarization via buckling of the cantilever, but the horizontal response is decoupled from the vertical polarization. Both images shown here were recorded in direct succession using the same PFM settings.

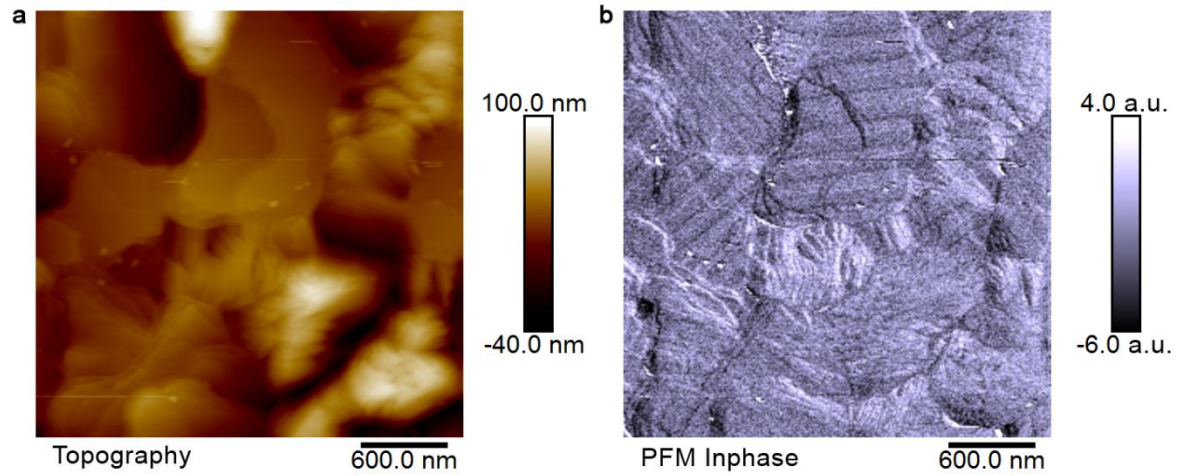

Fig. S3. (a) Topography and (b) PFM Inphase image of the same $MAPbI_3(Cl)$ grain after thermal annealing and without subduing the sample to solvent vapor. The flat grains show line-shaped domain structures.

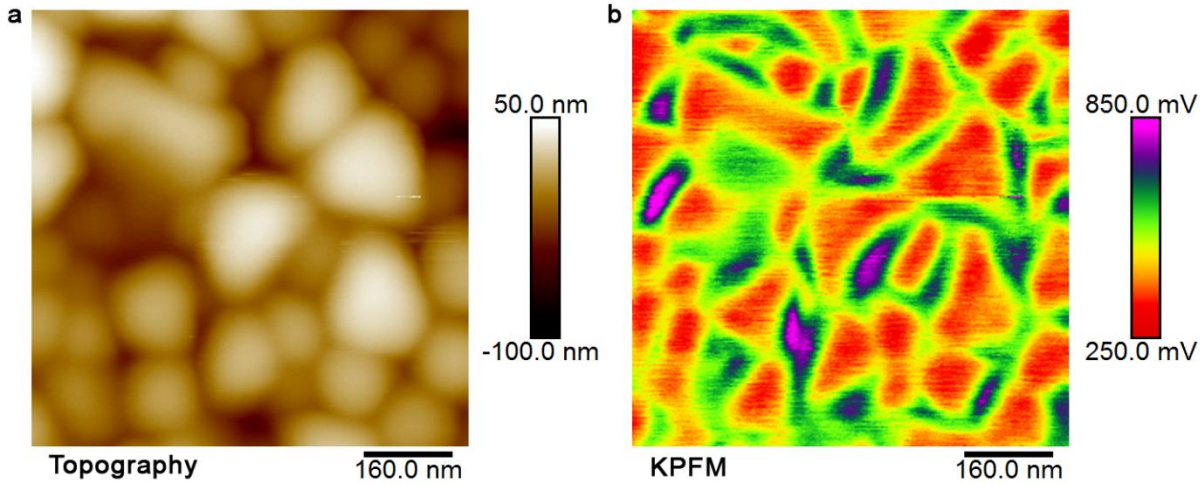

Fig. S4. (a) Topography and (b) KPFM image of the same $MAPbI_3(Cl)$ sample featuring small grains (prepared in air and after thermal annealing). Flanks of tilted cuboid grains exhibit high surface potential on flat grain flanks and low surface potential at rounded edges.

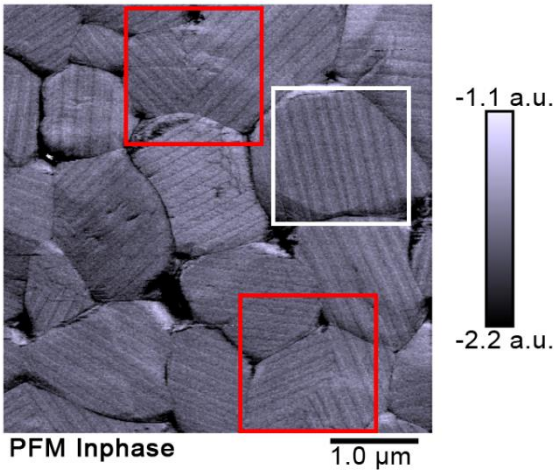

Fig. S5. PFM image of ferroelectric $MAPbI_3(Cl)$ domains on multiple grains show typical patterns of polarization: Some grains exhibit only one pattern of parallel domains (white square), whereas bigger grains often feature multiple areas of similar patterns, rotated approximately 90° relative to each other (red squares).

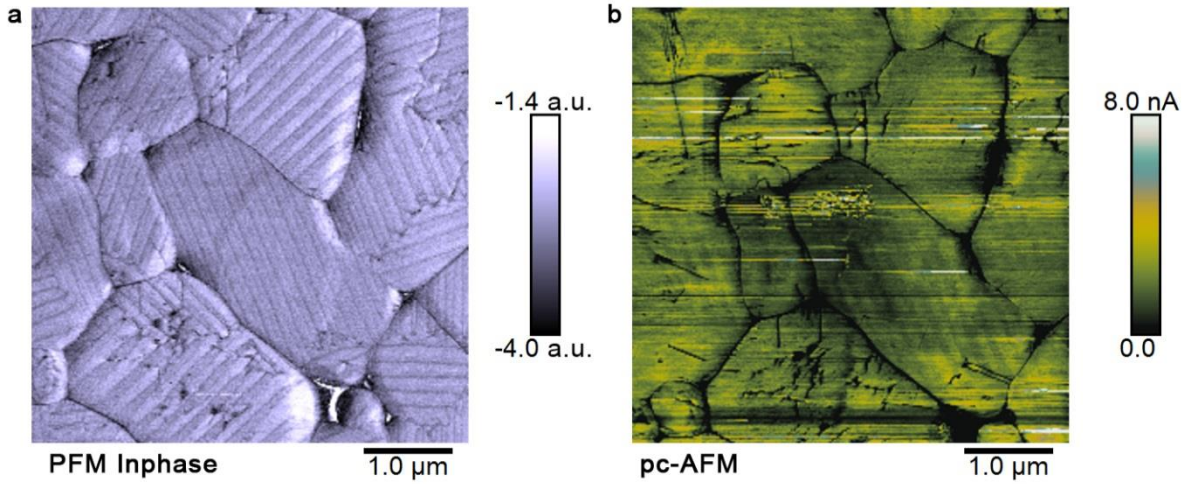

Fig. S6. (a) PFM image of Perovskite grains showing different ferroelectric domains and (b) pc-AFM image of the same grains showing the correlation of the local photo current with the ferroelectric domains.

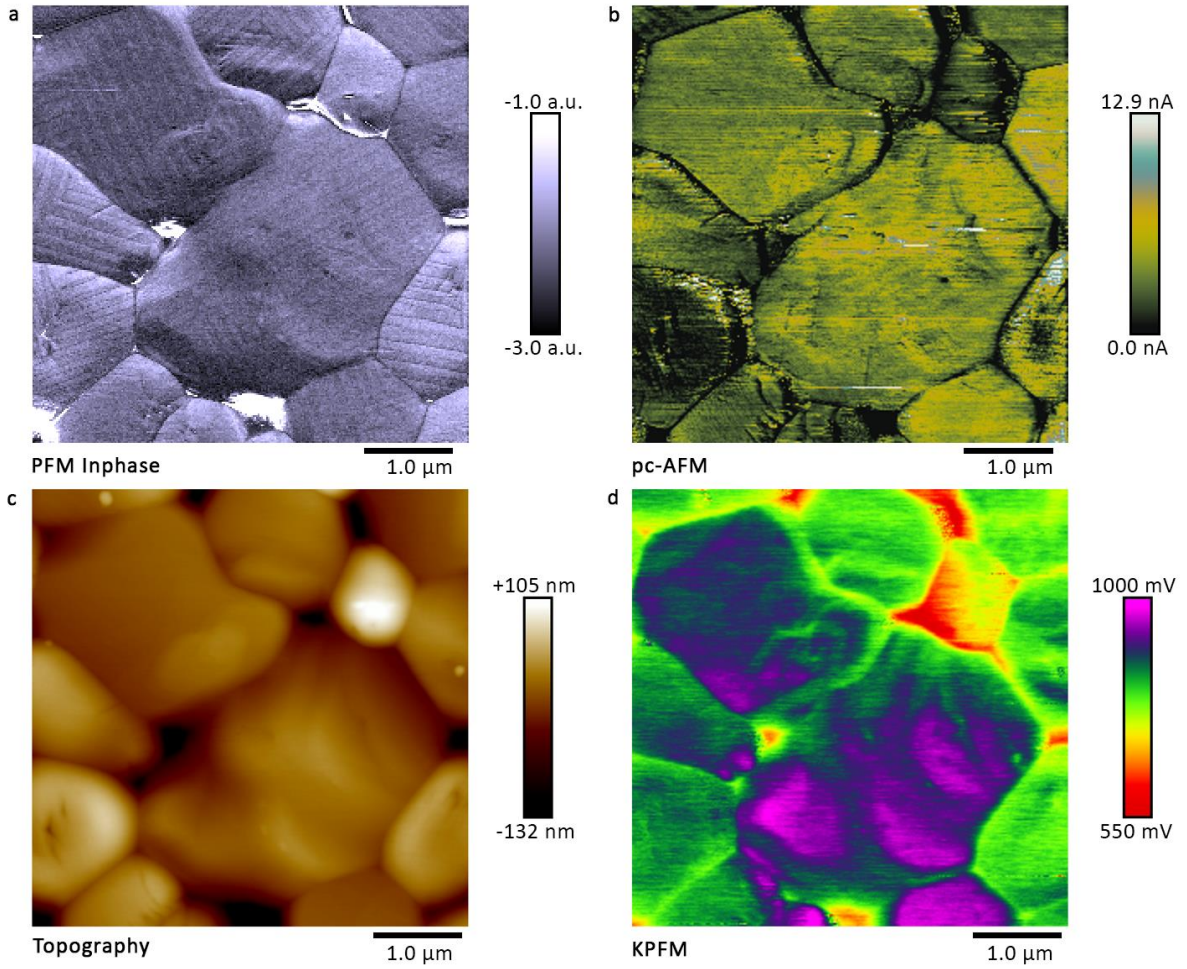

Fig. S7. (a) PFM, (b) pc-AFM, (c) topography and (d) KPFM images of the same flat $MAPbI_3(Cl)$ grain. This measurement was performed on a different sample than depicted in Fig. 2 or Fig. S7, yet shows similar grain properties. Neither topography nor KPFM are influenced by the ferroelectric domain patterns visible in the PFM measurements. The pc-AFM image, measured under short-circuit conditions, exhibits the same striped patterns as the PFM image, indicating an influence of the ferroelectric polarization on the local charge carrier extraction.

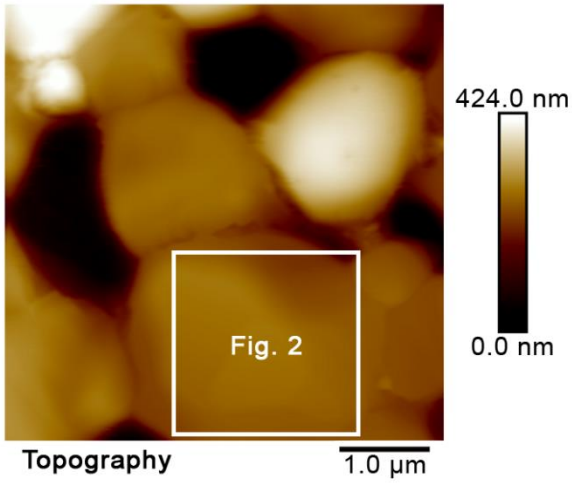

Fig. S8. 5 µm × 5 µm AFM topography image showing the environment of the grain depicted in Fig. 2.

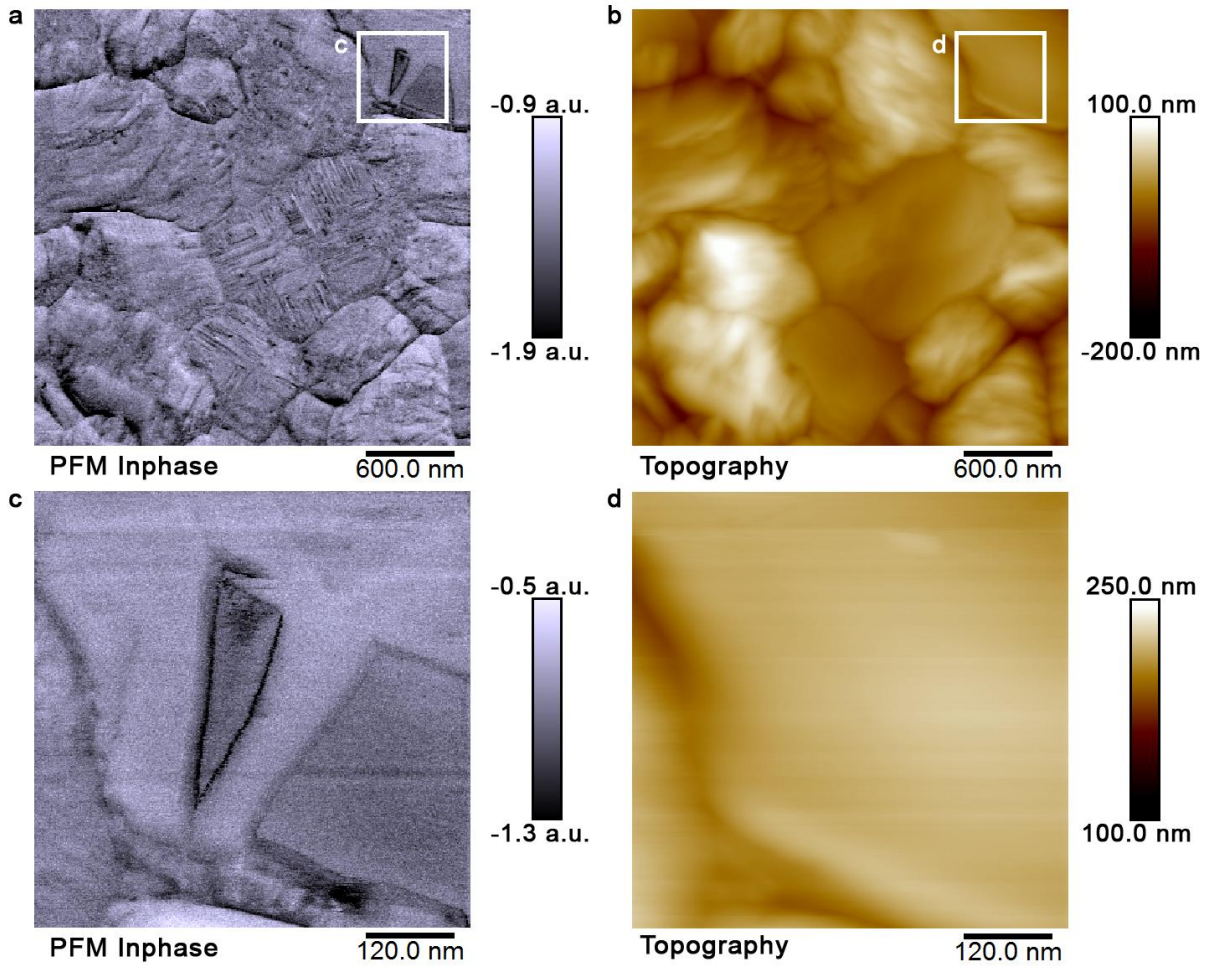

Fig. S9. $MAPbI_3$ thin-films solution deposited directly atop an ITO electrode (no PEDOT:PSS layer) omitting methylammonium chloride. Despite the different film forming in absence of methylammonium chloride, the distinct domain features prevail: (a) PFM image: The grains exhibit alternating ferroelectric domains as observed on $MAPbI_3(Cl)$ including various shapes and orientations. (b) The topography image shows a grain surface significantly rougher than $MAPbI_3(Cl)$ samples. (c)+(d) Detailed PFM and topography images show ferroelectric domains that are not visible in the sample topography of a flat grain.

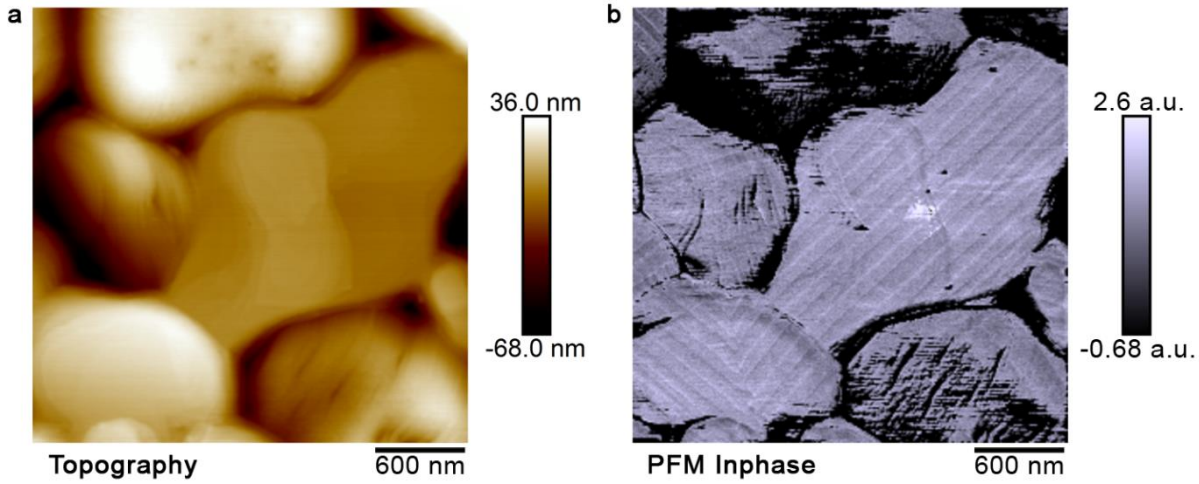

Fig. S10. $MAPbI_3(Cl)$ grains with a terrace-like surface topography show continuous domains extending over terrace flanks and hence different sample heights. The domains do not show any correlation with the shape of the terraces. While the PFM image exhibits some cross-talk from topography (central area in this image) the domain patterns are clearly distinguishable from topographical features.

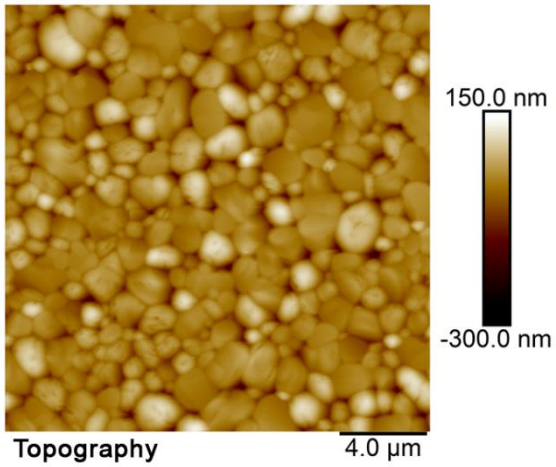

Fig. S11. Large area (20 µm × 20 µm) AFM image of a typical sample topography.

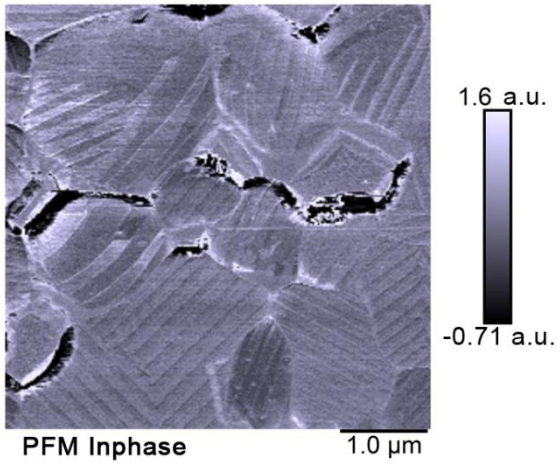

Fig. S12. PFM image of a sample region exhibiting rounded and tilted grains resulting in domain patterns of varying width and shape. The flat grains in the bottom half of the image show highly oriented domain patterns.

Settings for AFM measurements:

Figure S2a: horizontal, Figure S2b: vertical, 1500 mV AC bias, 34.37 kHz, scan angle 90°, probe SCM-PIC-V2. Figure S3: 1500 mV AC bias, 110.46 kHz, horizontal, scan angle 90°, probe SCM-PIC-V2. Figure S4: Drive amplitude 3000 mV, w/o illumination, probe SCM-PIT. Figure S5: 1500 mV AC bias, 33.14 kHz, vertical, scan angle 90°, probe SCM-PIC-V2. Figure S6a: 1500 mV AC bias, 33.98 kHz, vertical, scan angle 90°, probe SCM-PIC-V2. Figure S6b: under illumination, +800 mV bias, probe SCM-PtSi.
Figure S7a: 1000 mV AC bias, 53.09 kHz, vertical, scan angle 90°, probe SCM-PIC.
Figure S7b: under illumination, w/o bias, probe SCM-PIT. Figure 7c+d: Drive amplitude 3000 mV, w/o illumination, probe SCM-PIT.
Figure S9a+c: 1000 mV AC bias, 41.75 kHz, vertical, scan angle 90°, probe SCM-PIC-V2.
Figure S10b: 1500 mV AC bias, 109.97 kHz, vertical, scan angle 90°, probe SCM-PIC-V2.
Figure 12: 1500 mV AC bias, 62.0 kHz, vertical, scan angle 90° probe SCM-PIC.

Sample fabrication in Figure S9:

PbI_2 (Sigma-Aldrich) was dissolved in DMSO (250 mg/ml) and subsequently filtered with a hydrophilic membrane filter (pore size 0.25 µm). Then the solution was blade-coated on a cleaned ITO sample. After 20 s, the films were dried under nitrogen flow to obtain a smooth and homogeneous PbI_2 layer. The substrates were transferred into a glovebox with nitrogen atmosphere for spin-coating MAI that was dissolved in IPA (40 mg/ml) without any additives. Further process steps and parameters are identical to the $MAPbI_3(Cl)$ sample preparation as described in the Method section of the manuscript.